DIRC-based PID for the EIC Central Detector

T. Cao[3], T. Horn[1] (co-PI), C. Hyde[2] (co-PI), Y. Ilieva[3] (co-PI), P. Nadel-Turonski[4,*] (co-PI), K. Peters[5], C. Schwarz[5], J. Schwiening[5] (co-PI), H. Seraydaryan[2], W. Xi[4], C. Zorn[4].

[1)] The Catholic University of America, Washington, DC 20064
[2)] Old Dominion University, Norfolk, VA 23529
[3)] University of South Carolina, Columbia, SC 29208
[4)] Thomas Jefferson National Accelerator Facility, Newport News, VA 23606
[5)] GSI Helmholtzzentrum für Schwerionenforschung GmbH, 64291 Darmstadt, Germany
[*)] turonski@jlab.org

An essential requirement for the central detector of an Electron-Ion Collider (EIC) is a radially-compact subsystem providing particle identification (e/π, π/K, K/p) over a wide momentum range. To this end, the electromagnetic calorimeter needs to be complemented by one or more Cherenkov detectors. With a radial size of only a few cm, a Detector of Internally Reflected Cherenkov light (DIRC) is a very attractive option. Currently, R&D is being undertaken for several DIRC projects around the world (PANDA, SuperB, Belle-II). A future EIC DIRC can benefit from many aspects of this R&D, but it also provides its own unique set of challenges and priorities, in particular due to the higher momenta of the produced particles, and the impact of the readout of the DIRC bars on the required detector acceptance.

The key questions addressed by the proposed R&D include: developing a compact readout "camera" that can operate in the high magnetic field of the central solenoid, investigating the possibility to extend the momentum coverage (up to 50% beyond state-of-the-art for π/K identification) by improving the θ_c resolution, and studying the integration of a DIRC into the EIC full-acceptance detector with and without a supplementary gas Cherenkov detector.

This proposal is currently in its first year of funding. Following the recommendations of the advisory committee, the FY12 proposal extends the scope of the sensor testing program by broadening the collaboration and taking advantage of a new, dedicated test facility that JLab will set up as a contribution to the EIC detector R&D effort. This test facility includes a 5-T superconducting solenoid, previously used in Hall B for the DVCS program at 6 GeV.

1. Physics Requirements for Large-Angle PID

While an EIC will support multiple interaction regions, the primary detector will have a general purpose character that should offer satisfactory performance for a wide range of processes and kinematics. In practice, however, the most stringent PID requirements for the central detector come from semi-inclusive and exclusive reactions.

Kinematically, there are two features to consider. First, the asymmetry between the electron and ion beam energies tends to boost the produced hadrons to high lab momenta and small angles. This poses a challenge for the forward detection, but as shown in Fig. 1, the momenta of particles produced in Deep Inelastic Scattering (DIS) at central angles, are generally moderate if no additional constrains are applied.

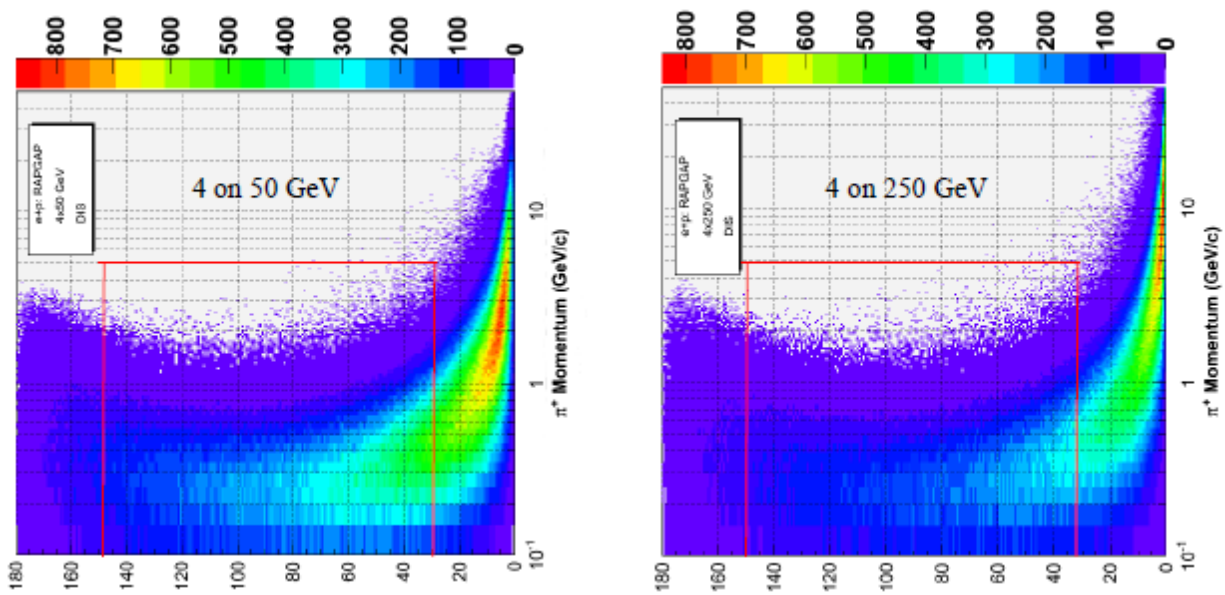

Figure 1: DIS pions produced in collisions of 4 GeV electrons on 50 and 250 GeV protons, respectively. The vertical red lines placed at 30° and 150° indicate the approximate transition from the central detector to the endcaps. The horizontal line at 4 GeV/*c* shows the limit of 3σ π/K separation for current DIRC detectors. No cuts on Q^2 have been applied in the plots. Note that in the HERA convention the electron beam is moving towards 180° (*i.e.*, towards the left) and the ion beam is moving towards 0° (*i.e.*, towards the right).

However, as exemplified in the following sections, the more exclusive the process, the more momentum tends to be picked up by the produced (leading) hadron. The resulting momentum *vs* angle distributions are thus different than the inclusive ones shown in Fig. 1, in particular if kinematic cuts are applied (for instance on Q^2).

1.1 Semi-Inclusive DIS and Transverse Momentum Distributions (TMDs)

Semi-Inclusive Deep Inelastic Scattering (SIDIS) is one of the best processes one can use to reveal the partonic structure of the nucleon. Two different factorization schemes allow to study different features of a complicated partonic picture. The traditional, collinear factorization scheme applies when the p_T of the produced hadron is of order Q and the intrinsic transverse momentum (k_T) of the quarks inside the

nucleon can be neglected. The transverse momentum of the produced hadron (p_T), then reflects only the dynamics of the process. In this approach, one benefits from studying values of $p_T \sim Q$.
However, if one wants to learn about the 3-D partonic structure of the nucleon, and ultimately the orbital angular momentum, the transverse momentum k_T becomes important. A different factorization scheme is required to include k_T explicitly. It is known as TMD factorization, and applies when $p_T \sim \Lambda_{QCD} << Q^2$. Employing polarized beams, the EIC will be able to study a number of TMDs. Each TMD represents different combination of spin and quark momentum correlations. One of the simplest TMDs, called the Sivers function, was suggested at the INT 10-3 program as a golden measurement for an EIC. The k_T-distribution for the Sivers function is shown in Fig 3.

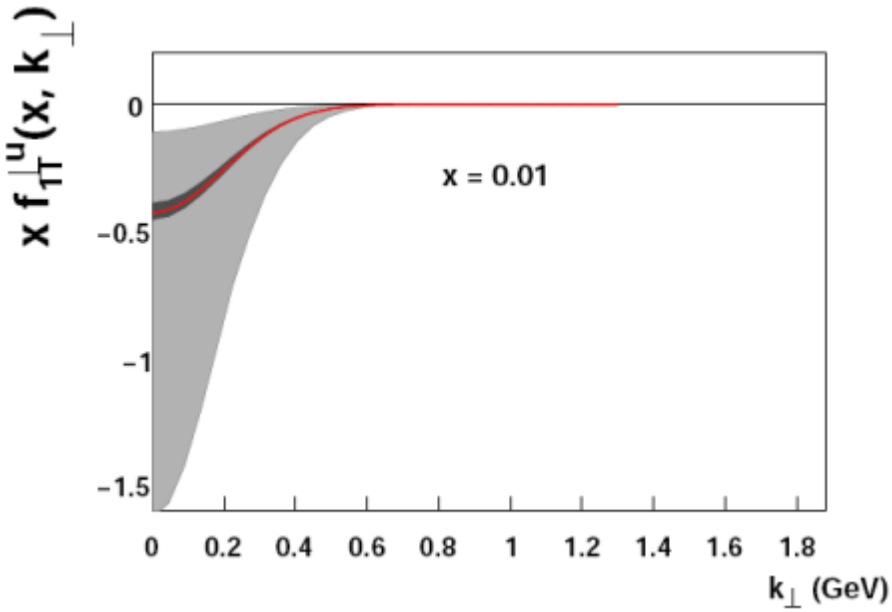

Figure 2: Dependence of the Sivers function on the transverse quark momentum. The light and dark grey bands are estimates of the uncertainty before and after EIC data become available, respectively.

The distribution shows three regions of interest. As expected from the natural momentum scale associated with the nucleon, TMDs are large only at low values of k_T (and hence low to moderate p_T). Although the shape of the TMDs may change with x, they will fall off rapidly at large k_T for all values of x. At high p_T, we know that the collinear picture applies and provides a good description of the data. Both the collinear and TMD factorization schemes will describe the same physics in a transition region of moderate p_T and relatively large k_T that contains the tail of the TMDs. To understand the TMDs one would thus want to map out both the region of low k_T where they are dominant, as well as the completely unknown transition region for which the EIC will provide the first data.
By splitting up k_T into its components, we obtain an image in the transverse plane (with respect to the virtual photon direction). Figure 3 shows how the incoming photon "sees" the motion of the quarks.

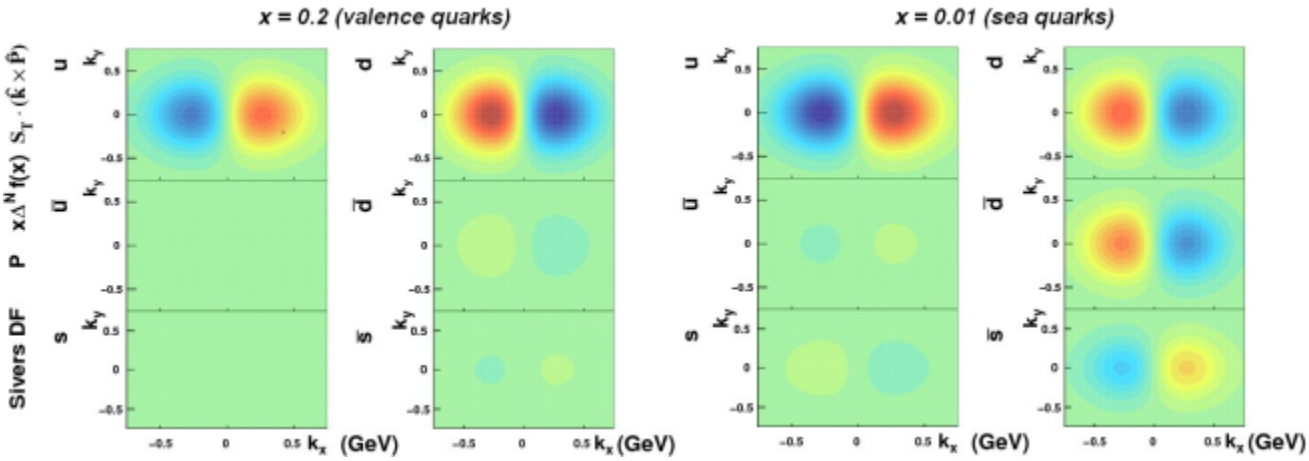

Figure 3: Sivers function for u, d, and s quarks (as well as antiquarks) as function of the transverse quark momentum components as "seen" by the incoming photon. Red indicates an excess and blue a depletion. Flavor separation will require π/K identification.

The flavor separation shown in Fig. 3 will, of course, require appropriate particle identification. However, one needs to keep in mind three things. First, it is the transverse momentum component of the produced leading hadron (p_T) rather than the quark momentum k_T that is the actual observable. Depending on the kinematics of the process, p_T is usually larger than k_T. In order to disentangle the two, the measured range in p_T has to significantly exceed the desired range in k_T. Second, as noted above, both k_T and p_T are defined in the ion rest frame with respect to the virtual photon direction (rather than that of the ion beam). The p_T in the lab frame is thus boosted along the beams direction, and tends to differ from the p_T in the target rest frame. And finally, due to the boost and the meson scattering angle, the lab momentum p, which is the parameter determining the coverage of the PID detectors, is almost invariably larger than the p_T in the ion rest frame (thus, if one is limited by p, one can generally extend the coverage in k_T somewhat by going to lower ion beam energies). The lab angles and momenta as function of p_T for the SIDIS leading hadron at intermediate collision energies are shown in Fig. 4.

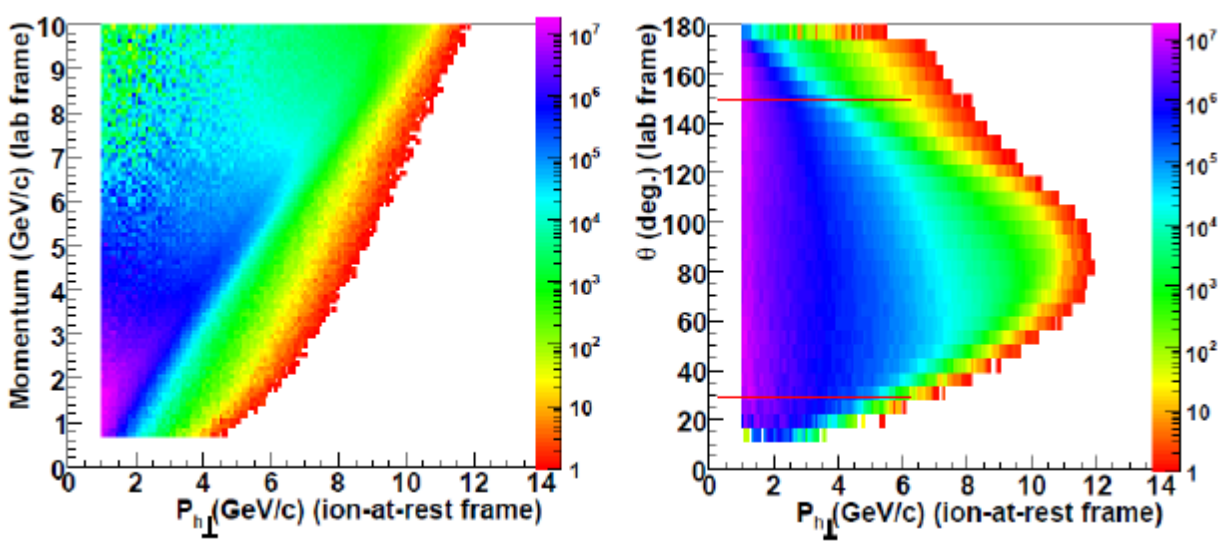

Figure 4: Leading SIDIS pions for 11 electrons on 60 GeV protons, with cuts on $0.2 < z < 0.8$, $Q^2 > 1$ GeV^2, $M_x > 1.6$ GeV, $W > 2.3$ GeV, $0.05 < y < 0.8$, and $p < 10$ GeV, as function of p_T. The horizontal red lines indicate the approximate transition from the central detector to the endcaps.

The SIDIS lab momenta as a function of angle are shown in Fig. 5. The left panel focuses on the central detector, indicating the coverage of a DIRC (both state-of-the-art and "Super-DIRC"). The right panel shows the distribution of forward-going particles, the momenta of which are driven by the ion beam energy. Due to the lower electron energy in the right panel, the momenta of backward-going mesons are lower than on the left panel.

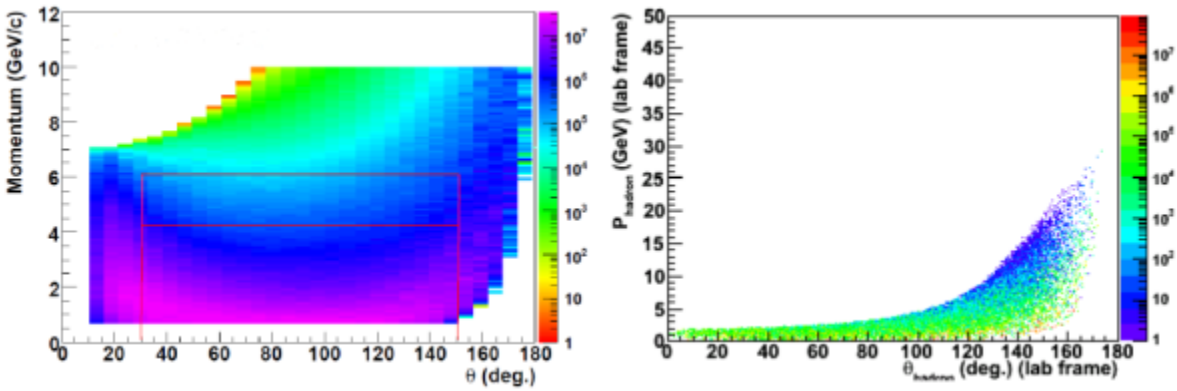

Figure 5: Leading SIDIS pions for 11 GeV electrons on 60 GeV protons (left panel) and 4 GeV electrons on 50 GeV protons (right panel). In the left panel the same cuts have been applied as in Fig 4, while on the right, $0.4 < z < 0.6$ and $1 < Q^2 < 10$ GeV^2. The horizontal red lines at 4 and 6 GeV/c indicate, respectively, the 3σ π/K separation of a state-of-the-art DIRC and a the upper limit of a possible "Super-DIRC". Note that these and subsequent plots use the standard electron scattering convention where the electron beam moves towards 0°. The left/right directions of the electron/ion beams are, however, the same as in Fig. 1.

Ideally, one would like to have the EIC detector provide flavor separation over the full range of p_T accessible in SIDIS. However, for studies of TMDs such as the Sivers function, one absolutely needs to cover a range in p_T that will make it possible to disentangle the lower end of the k_T distribution. But it would also be highly desirable to cover the hitherto unknown transition region at intermediate p_T (and high k_T) where both TMD- and collinear factorization is relevant. Unfortunately, the fact that this region is poorly known also makes it difficult to formulate a very precise requirement at this time. More theoretical studies are needed. Nevertheless, it would seem that pushing π/K identification beyond the maximum lab momentum (p) of 4 GeV/c offered by a BaBar-type DIRC (or an aerogel RICH) would be significant. This could be accomplished with a "Super-DIRC", capable of reaching 5 - 6 GeV/c, or by adding a supplementary low-threshold gas Cherenkov detector. The latter could extend the maximum lab momentum to 9 GeV/c, but it would require at least 60 - 70 cm of radial space in addition to the few cm needed for the DIRC.

Further increases in coverage are possible (for instance by replacing the threshold gas Cherenkov by a RICH detector, preferably with two radiator gases), but would come at a hefty price both in dollars and

radial space, for which the PID detector competes with other systems. Flavor separation over the full p_T range thus seems unfeasible for the primary EIC detector, in particular for a stage-II machine. The focus of this proposal is thus to present a solution that could accommodate the PID needs of the TMD program, and provide a substantial coverage of the general SIDIS kinematics.

1.2 Exclusive reactions and Generalized Parton Distributions (GPDs)

Measurements of the transverse spatial parton distributions, using the GPD framework, are complementary to the 3-D imaging in momentum space discussed in the previous section. Experimentally, the exclusive sector is more complicated in the sense that one not only needs to detect and identify the leading meson (which originates from the struck quark), but one would also like to use a suite of distinct channels, including both diffractive (no change in quantum numbers, *e.g.*, DVCS, φ, J/Ψ) and non-diffractive (with a change in quantum numbers, *e.g.*, π, K, ρ^+) processes. Comparisons of parton distributions in transverse impact-parameter space are illustrated in Fig. 6.

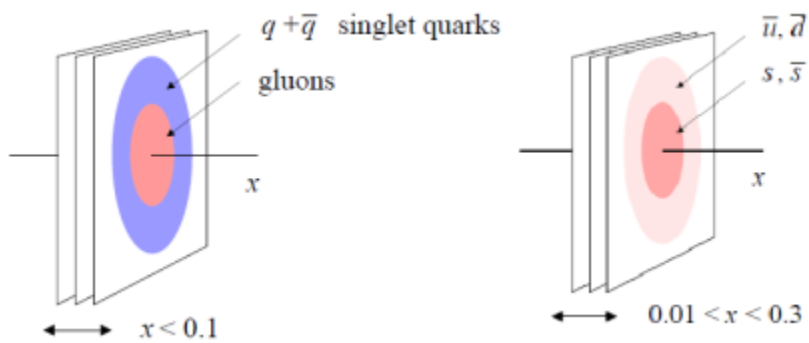

Figure 6: A comparison between, for instance, DVCS and J/Ψ production can teach us about the relative quark and gluon radii of hadrons, while a comparison between pions and kaons (or non-diffractive vector meson channels) can tell us about the relative distributions of light and strange sea quarks.

Since decaying mesons split their momentum between the decay products, and often have a relatively narrow invariant mass (*e.g.*, the φ), at any given c.m. energy they tend to pose less of a detection challenge than long-lived pseudoscalars. But the latter are, on the other hand, mostly of interest for exploring the sea at values of x corresponding to the "pion cloud", and hence do not require the highest beam energies.

There is also an important difference between light and heavy mesons (such as the J/Ψ). The latter are always produced in small-size configurations, and thus do not rely on high Q^2 to ensure that factorization applies, enabling an interpretation in terms of GPDs. However, since high-Q^2 production is associated with large meson angles in the lab frame, light mesons are a good illustration of the PID requirements for the central detector. Figure 7 shows the angular distribution of exclusive light mesons at several c.m. collision energies, all with a high Q^2 (> 10 GeV^2) cut applied.

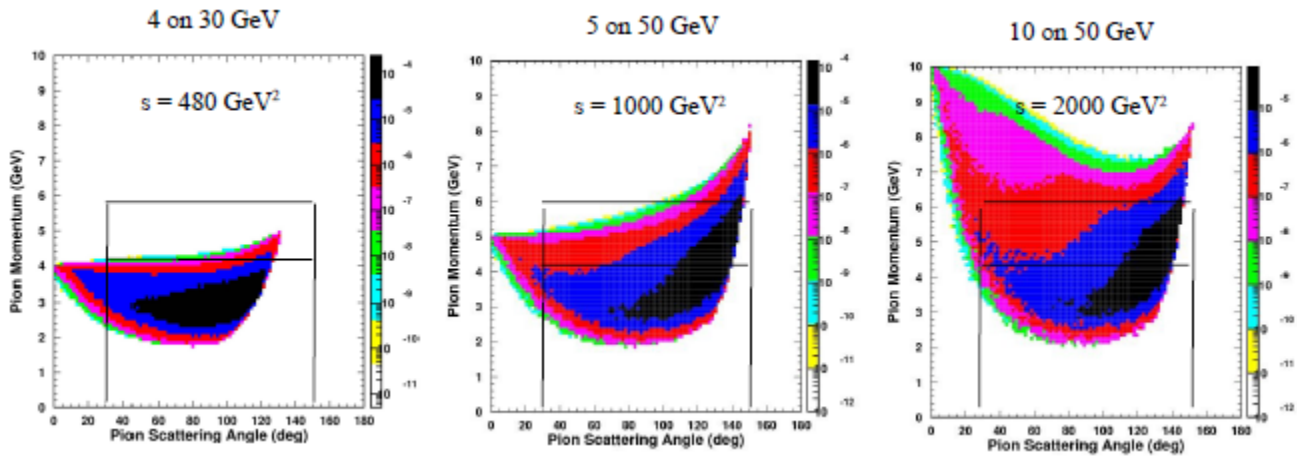

Figure 7: Exclusive pion production at Q^2 > 10 GeV^2 for three kinematics: 4 on 30, 5 on 50, and 10 on 50 GeV. As indicated by the horizontal lines, π/K identification up to 4 GeV/*c* is sufficient at the lowest c.m. energies, but quickly becomes inadequate as the energy increases.

A momentum coverage up to 4 GeV/*c* (state-of-the-art DIRC) is only adequate for the very lowest values of *s*. Increasing this value to 6 GeV/*c* (the "Super-DIRC" limit) would provide full coverage up to s = 2000 GeV^2, if the collision kinematics is reasonably symmetric, and partial coverage for higher energies. Pushing this limit to 9 GeV/*c* (using a supplementary low-threshold Cherenkov detector), would give good coverage for proton energies approaching 100 GeV, at which point the cross section for non-diffractive channels would in any case become very small.

1.3 e/π and p/K identification

While the previous sections focused on π/K identification, both e/π and, to some extent, p/K capabilities are also important for the EIC central detector. The former is essential for reliably detecting and identifying high-Q^2 electrons when the electron beam energy is low, and the energy of the scattered electrons is even lower. Fig. 1 also indicates that the pion background may be significant for momenta up to about 1 GeV/*c*. A DIRC, and in particular a "Super-DIRC", would be able to augment the capabilities of the electromagnetic calorimeter in this range. The ability to push the lower limit of reliable electron identification can be important for measuring F_L, as well as for other measurements that wish to cover a wide range of photon virtualities (Q^2) and electron inelasticities (y). A supplementary low-threshold gas Cherenkov detector would extend the e/π separation up to about 3 GeV/*c*. However, since the pion background drops off rapidly in the 1 - 3 GeV/*c* range, the benefits from this additional coverage need to be determined.

A gas Cherenkov detector would offer only p/K identification above the kaon threshold (~ 9 GeV/*c*), but a DIRC could cover a significant range at lower momenta. Already a BaBar-type DIRC can do a good job up to about 6 GeV/*c*, while a "Super-DIRC" would extend this even further. High-p_T protons and antiprotons are expected to be relatively uncommon, as most nuclear spectators and baryons originating from the fragmentation of the target nucleon will be produced at small angles and hit the endcap detectors. Still, the capability to detect and identify high-p_T protons can be valuable.

2. Proposed R&D

2.1 Development of a Compact DIRC readout "camera" for high magnetic fields

Hermeticity is a key design goal of the EIC detector, and thus there are only limited possibilities to accommodate a large inactive volume inside the detector, or to give up significant angular coverage in the endcaps. While the radius of the central tracker is important for the momentum resolution of particles produced at large lab angles, a good tracking resolution at forward rapidities primarily requires a strong solenoidal field. The readout for a DIRC should thus be able to operate in magnetic fields of up to 2 - 4 T (the exact specifications for the solenoid are yet to be determined), and be reasonably compact. Figure 8 shows the baseline layout for the EIC detector.

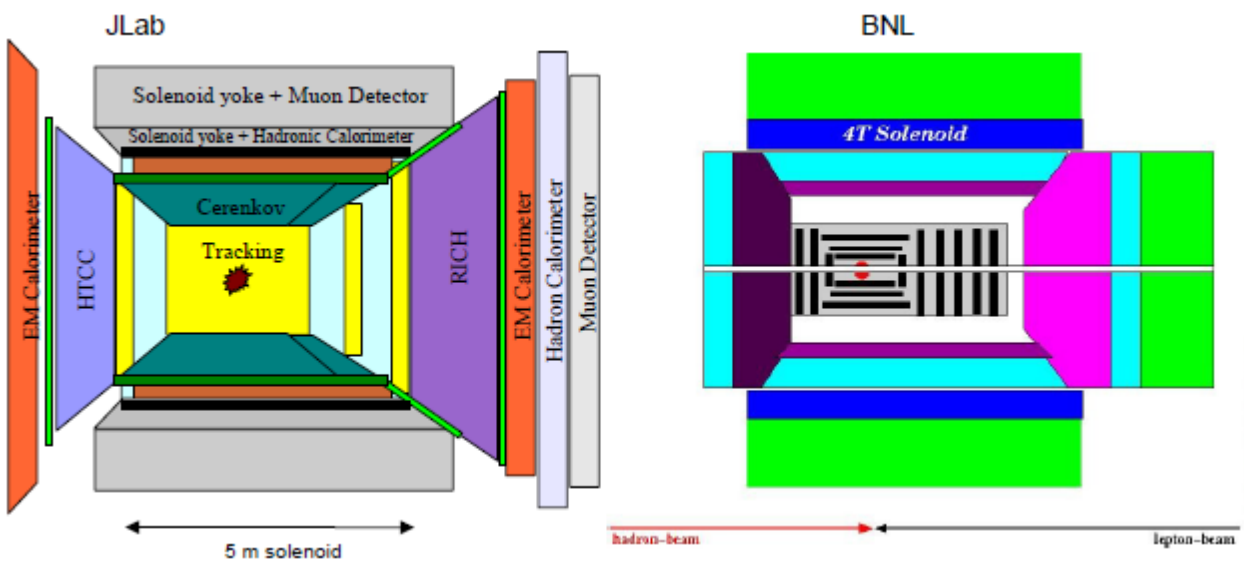

Figure 8: Baseline EIC central detector cartoon as shown at INT-10-3. The JLab version on the left has the DIRC and TOF in the barrel colored dark green, while the BNL version on the right is purple. The readout will replace the last 20 - 30 cm of the DIRC bar so as not to interfere with the electron tracking. The BNL layout is generally similar, but does not explicitly show any gas Cherenkov in the barrel.

The expected PID performance of the DIRC is determined by the resolution in θ_c, the polar opening angle of Cherenkov light emitted from the particle traversing the detector. The angle θ_c is defined as $\cos\theta_c = 1/n(\lambda)\beta$, where $\beta = v/c$, v is the particle velocity and $n(\lambda)$ is the index of refraction of the material. In a dispersive medium, the latter is a function of λ, the wavelength of the Cherenkov photon.
The uncertainty of the Cherenkov angle for a particle track, σ_c^{track}, behaves as

$$(\sigma_c^{track})^2 = (\sigma_c^{photon} / \sqrt{N_{p.e.}})^2 + (\sigma^{track})^2,$$

where $N_{p.e.}$ is the number of detected photoelectrons and σ_c^{photon} is the single-photon Cherenkov angle resolution. The last term, σ^{track}, is the uncertainty of the track direction in the DIRC, dominated by

multiple scattering and the resolution of the tracking detectors.
The single-photon Cherenkov angle resolution σ_c^{photon} can be calculated as

$$\sigma_c^{photon} = \sqrt{\sigma_c^{pixel} + \sigma_c^{bar} + \sigma_c^{imperfections} + \sigma_c^{chromatic}}$$

where σ_c^{pixel} is the contribution from the detector pixel size, σ_c^{bar} is the uncertainty due to optical aberration and imaging errors, $\sigma_c^{imperfections}$ is the uncertainty due to bar imperfections (such as non-squareness), and $\sigma_c^{chromatic}$ is the uncertainty in the photon production angle due to the dispersion n(λ) of the fused silica material.
The readout "camera" consists of an expansion volume (EV) with attached sensors. The purpose of the expansion volume is to project a spatial image of the Cherenkov light from the DIRC bar onto the sensors. Using sensors with a smaller pixel size makes it possible to reduce the size of the expansion volume, or to improve the spatial resolution of the image. The size of the expansion volume can also be reduced by introducing active focusing elements (lenses or mirrors), although careful design and testing is required to minimize photon losses.
The size of the expansion volume planned for the PANDA barrel DIRC is 30 cm, both radially and along the beam axis, while SuperB plans to have one that has a radius of 56 cm and a length of 22 cm. Due to its large radius, the SuperB EV would be challenging to integrate with the EIC detector. Since an important goal of the R&D is to improve the DIRC performance beyond state-of-the-art, and there is a tradeoff between size and resolution, we expect the EIC expansion volume to be only a little smaller than the one planned for PANDA.
The next generation of sensors that will be used in the EIC DIRC needs to have a large number of small pixels and a high tolerance to magnetic fields. However, for the proposed R&D it is cheaper and more efficient to use two sets of sensors, testing two types of technology. One set will provide a sufficient number of pixels for use with the expansion volume prototype to optimize the reconstruction of the projected image (MCP-PMTs), the other set is expected to have a high magnetic-field tolerance (SiPMs). Both types of sensors will be tested in strong magnetic fields.

2.1.1 Compact expansion volume

The required depth of the expansion volume is given by the size of the detector pixels, the size of the bar image after focusing, and the desired Cherenkov angle (θ_c) resolution. In order to reduce the EV size and to simplify operations, the water used in BaBar was replaced with oil for PANDA and with fused silica for SuperB. The latter would probably be the preferred choice for the EIC.
In the EIC design we will also try to improve performance while maintaining a compact size by introducing an active focusing element, such as a lens doublet. However, please note that a compact design along the lines of Belle-II, relying primarily on precise timing while sacrificing spatial image resolution, would be unlikely to fulfill the requirements of the EIC in terms of momentum coverage and the length of the DIRC bars.

2.1.2 Small-pixel readout

A small pixel size is essential for reaching the desired spatial resolution. To test the performance in a prototype, a sufficient number of channels is required. The most economical way of achieving this is to use multi-pixel PMTs such as the Hamamatsu H9500-03 (256 pixels, 3.0 mm pixel pitch) or Photonis

XP85022 (1024 pixels, 1.6 mm pixel pitch). An important performance consideration is optical and electrical cross-talk between pixels. A prototype of the Photonis 85022 tested at SLAC in 2005/2006 did not perform as well as a prototype of the Hamamatsu H9500.

2.1.3 Readout in a high magnetic field

Tests will be performed using SiPMs (aka Geiger-mode Avalanche Photodiodes, G-APDs) and MCP-PMTs with small-diameter MCPs, such as the 6-μm MCP-PMT produced by BINP, Novosibirsk. While SiPMs potentially could be less sensitive to magnetic fields, their high dark count rate (~ 1 MHz/cm^2 at room temperature) will require cooling to reach the desired performance.

The advisory committee suggested to join efforts with C. Zorn after he completes his one-year, FY11 project to test improved radiation-tolerant silicon photomultipliers. Consequently, the scope of the high magnetic-field testing of MCP-PMTs and SiPMs during years 2 and 3 has been significantly expanded. To support this effort, as well as future EIC-related sensor tests, a dedicated test facility will be set up at JLab. A detailed description of the facility and test plan can be found in Appendix A. The expanded sensor program has also brought new collaborators to this proposal.

2.1.4 Readout outside of the magnetic field

Following the recommendations of the advisory committee, we will also investigate the option of having very long DIRC bars penetrate the electron endcap and iron. Moving the readout to the outside would greatly reduce the requirements on compactness and magnetic-field tolerance. It would also give easier access to the sensors if they would need replacement, for instance due to radiation damage. However, the impact on detector integration and the overall performance of the endcap detectors could be significant.

2.2 Initial Development of a High-Performance DIRC

The primary goal of developing a “Super-DIRC” that would push the performance beyond the state-of-the-art, is to eliminate the supplementary gas Cherenkov detector, thereby reducing the radial space required for PID by at least 60 - 70 cm. The freed space can be used for a larger central tracker, which would improve the momentum resolution at large angles, or to reduce the radius of the solenoid magnet. A smaller overall radius would not only reduce the cost of the solenoid and the electromagnetic calorimeter, but also that of the endcap detectors (which goes as the radius squared). A cartoon of a configuration using only a “Super-DIRC” is shown in Fig. 9.

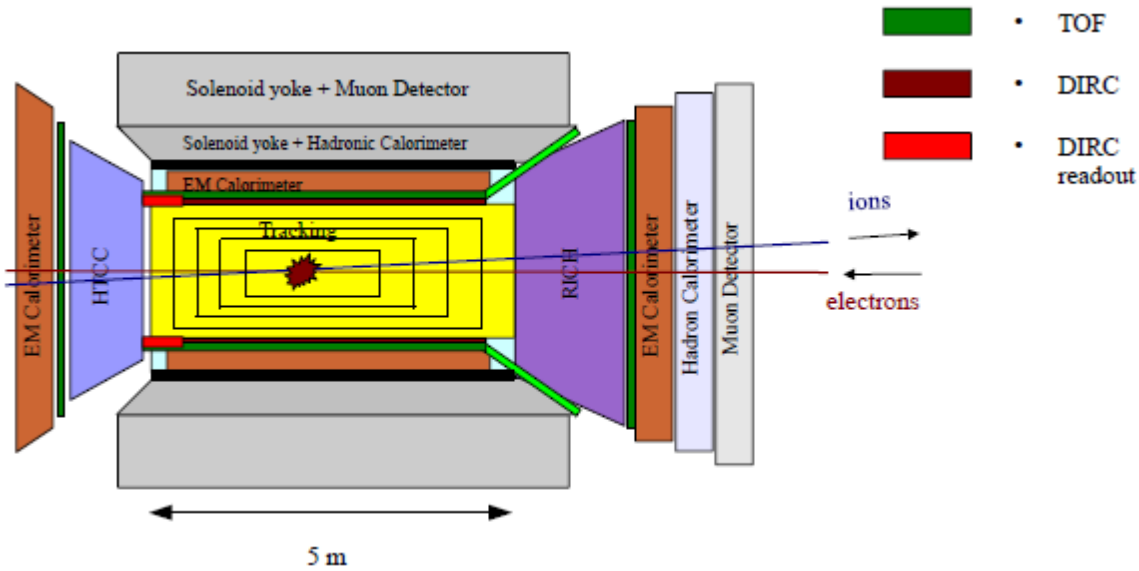

Figure 9: EIC central detector cartoon showing a DIRC-only configuration.

As the particle momentum increases, so do the demands on the Cherenkov angle resolution. Figure 10 shows how the π/K difference in Cherenkov angle drops from 6.5 mrad to 2.9 mrad between 4 GeV/*c* and 6 GeV/*c*. In an EIC, the pion background for kaons varies with reaction and kinematics, but is typically about 3:1. The usual 3σ criterion thus seems relevant for estimating the momentum range where the π/K identification is adequate. Achieving 3σ separation using radiator bars of fused silica would require a Cherenkov angle resolution of 1.3 mrad at 5 GeV/*c* and 1.0 mrad at 6 GeV/*c*. In addition to the challenges related to the design of the DIRC itself, achieving this performance also assumes that the central tracker will be able to provide an angular resolution at the mrad level (*i.e.*, comparable to the CLAS12 forward detector).

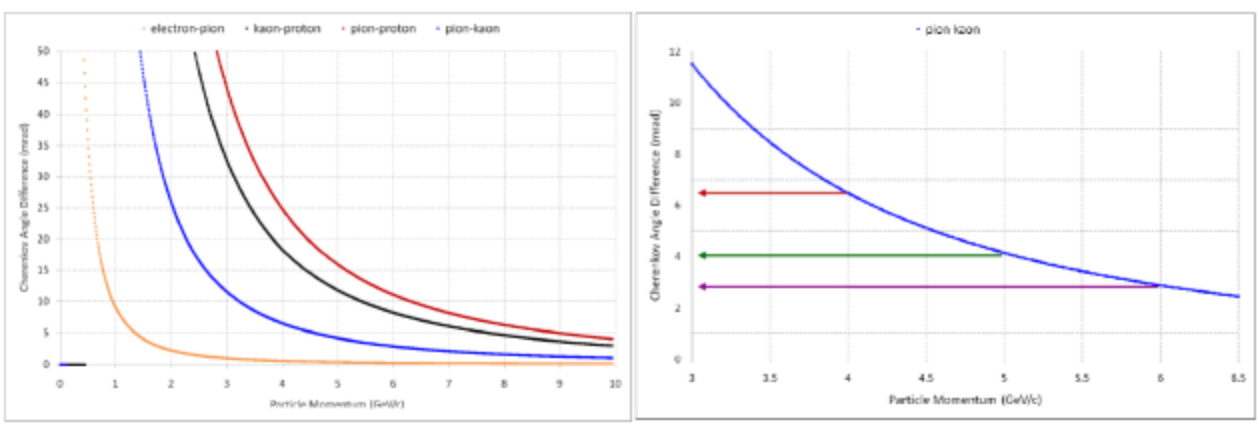

Figure 10: Cherenkov angle difference in fused silica as a function of momentum for e/π, π/K, K/p, and π/p (left panel), and a close-up of the π/K curve (right panel). Extending the π/K separation from 4 to 6 GeV/*c* requires more than a factor-of-two improvement in the angular resolution.

As shown by the equations above, there are four ways of improving the Cherenkov angle resolution:

1. Reducing the size of the image from the DIRC bar using focusing optics.
2. Reducing the pixel size of the readout to better resolve the image.
3. Improving the photon yield and collection (various methods).
4. Reducing the effect of chromaticity ($n = n(\lambda)$) through precise timing or wavelength filters.

The first two items are addressed in Section 2.1 above, as part of the readout optimization process.

2.2.1 Increasing the photon yield

The most straightforward way to improve the photon yield is to increase the bar thickness. This does not impose any additional manufacturing complications, but simulations are needed to study the impact of having 0.2 r.l. or more of bar material in front of the electromagnetic calorimeter and other subsystems. We will also investigate the possibility of reducing photon losses by using either MCP-PMT or MaMPT with an improved, UV-optimized photocathode, or large-cell SiPMs (due to their intrinsically high photon detection efficiency, PDE). The same SiPMs could be used for this purpose as for the magnetic field tests in section 2.1.3. Another way, falling outside the scope of the proposed R&D, would be to apply anti-reflective coatings to the optics in the focusing system to prevent losses in the glass/air boundary.

2.2.2 Precision timing

In a DIRC design with focusing optics and small-pixel readout the chromatic dispersion may no longer give a negligible contribution to the single-photon θ_c resolution. The focusing DIRC prototype at SLAC has shown that dispersion effects can be corrected by using fast timing at the 100-ps level, and this proposal thus aims to test the impact of timing close to that level. Should this prove not to be sufficient, more stringent timing requirements may be needed for the EIC DIRC, or wavelength filters can be applied to improve the single-photon resolution. The loss of photons due to the latter may, however, make the overall θ_c resolution for the track worse.

2.3 Investigation of PID based on a DIRC / gas Cherenkov combination

If the EIC central detector will be required to provide e/π and π/K discrimination over a wider momentum range than can be achieved with a state-of-the-art DIRC alone, one can augment it with a gas Low-Threshold Cherenkov Counter (LTCC), or replace it with a dual radiator (aerogel + gas) barrel RICH (which would be comparable with the DIRC / LTCC combination, but slightly larger and would offer slightly lower performance). The DIRC / LTCC alternative can have two configurations. Option 1, shown in Fig. 8, involves placing the DIRC outside of the gas Cherenkov, close to the time-of-flight (TOF) detectors. Option 2, shown in Fig. 11, places the DIRC inside of the gas Cherenkov close to the central tracker.

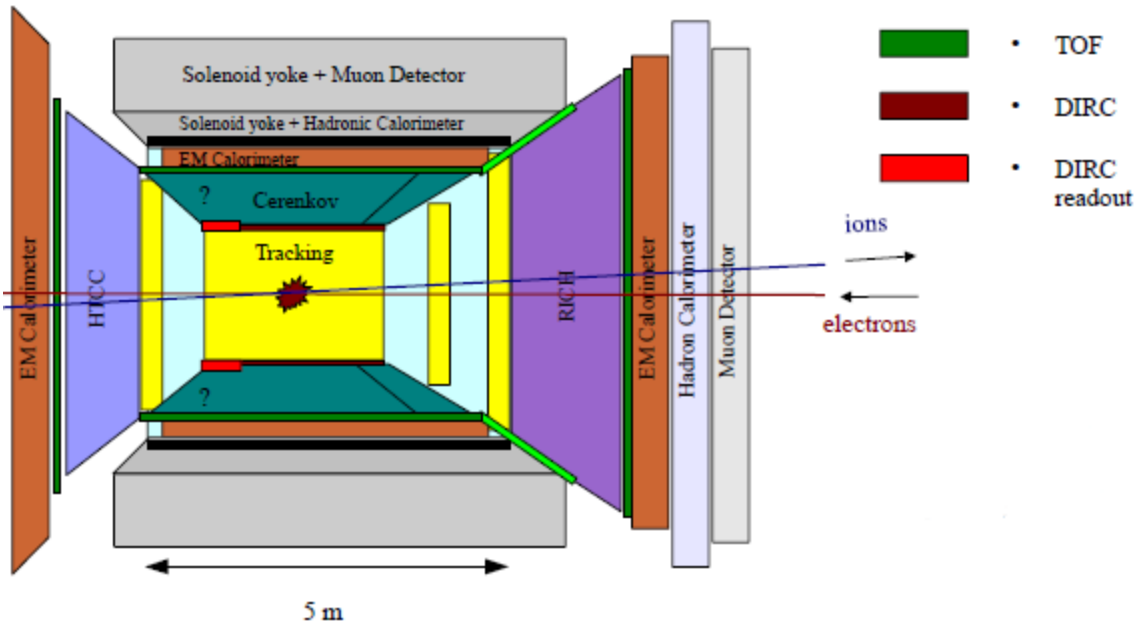

Figure 11: Detector cartoon showing the DIRC inside of the supplementary gas Cherenkov (Option 2).

Compared with Option 1, Option 2 has three main advantages:

1. Reducing the radius (and length) of the DIRC makes it significantly less expensive.
2. The proximity to the central tracker gives a better angular resolution for the incident track.
3. The shorter DIRC bar will suffer less from chromatic dispersion and will offer better timing.

There are, however, also some disadvantages:

1. Adding 0.15 - 0.20 r.l. of material in front of the gas Cherenkov will expose it to δ-electrons.
2. The proximity to the collision point will increase the solid angle covered by the expansion volume.
3. The increased distance to the TOF will reduce the timing benefits of the TOF detector.
4. It would not allow extending the DIRC bars outside of the endcap as they would interfere with the electron tracking at intermediate angles.

Option 1 seems to be the more conservative choice, but a quantitative study is needed to determine the feasibility of Option 2.

We thus propose to make a GEANT-based simulation of the central detector to compare the options above, understand the interdependence of the PID detectors, and optimize the parameters for various components, such as the thickness of the DIRC bars.

2.4 Background simulations

An important consideration for the choice between the DIRC-only or DIRC/gas-Cherenkov configurations is whether the electromagnetic calorimeter will be sufficient for dealing with the pion background outside the e/π identification range of the DIRC, or a sufficiently high threshold can be imposed on the detected electron without limiting the accessible kinematics. Electron identification is not only important for event reconstruction, but also for the asynchronous trigger, for which the scattered electron provides an excellent time stamp. A detailed knowledge of the pion background in the central

detector is thus essential for the choice of PID strategy.
To verify the validity of the 3σ separation criterion for various particle / background combinations over different channels and kinematics is a major undertaking. We hope to complete some of these studies ourselves, but will also try to compile results from collaborators at both labs and from universities involved in EIC simulations. Such input would allow to better quantify how the PID systems would perform for specific measurements.
An important consideration for all sensors inside the central detector, including those for a DIRC, are the expected background levels, in particular from neutrons, generated in the accelerator by residual gas, synchrotron radiation, *etc.* While the modeling of machine backgrounds goes beyond the expertise of our collaboration, we are working with an expert from SLAC (Mike Sullivan), who is currently reviewing the JLab design, and we hope to get similar input from experts at RHIC.

2.5 Synergies with Ongoing DIRC R&D

The hardware R&D makes substantial use of synergies with the PANDA DIRC detector development, both in terms of available hardware components and experience gained during the production of prototypes for bars, plates, and expansion volumes.
An example is the use of radiator bars made from synthetic fused silica. The production of a bar with optical quality sufficient for the EIC DIRC prototype would require a minimum of 4 - 8 bars to be produced at a cost of approximately $25k - $30k per bar. However, a number of prototype bars were produced for the PANDA Barrel DIRC R&D at GSI. The EIC DIRC R&D will have access to one of the bars for a possible test beam run.
Another example is the test of photon sensors. The GSI group owns a $10k electronic pulser and a $15k fast laser pulser system (PiLas) with a FWHM timing jitter below 25 ps, required for measurements of the fast single photon timing for the EIC DIRC. The test of SiPMs will require the sensors to be cooled to between -10° and -25° C. For simple tests a Peltier-cooled setup will be constructed at a modest cost. For more detailed studies the R&D will make use of a $10k large cooling box owned by the GSI group.
A software package for ray-tracing Cherenkov photons in DIRC radiators, developed at GSI, is currently being ported to the JLab computing environment for EIC DIRC R&D.

2.6 Detector Prototyping

In response to the advisory committee's recommendations the detector prototype plan has been divided into several stages with a focus on simulation in the early stages, and prototype construction and tests at the later stages. These stages are reflected in the R&D timeline and procurement plan.
In the first stage, the prototype will be implemented in a detailed detector simulation, initially using stand-alone ray-tracing software and later GEANT, to determine the preferred geometry of the expansion volume (EV) of the first prototype. The goal is to determine the optimum size and shape of the EV to match the size of radiator and detector pixel, and obtain the single photon Cherenkov angle resolution required for the EIC DIRC performance.
In the second stage, the output from the prototype simulation will be used to design and construct the first prototype, which should comprise a radiator bar, multi-pixel readout, and a small EV in a dark box suitable for transport and placement into a particle beam. Measurements in a test beam will be compared to the expected performance from simulation.
In the third stage, the simulation will be tuned to reproduce the data observed in the test beam and to update the DIRC design to reflect the performance requirements obtained from a detailed simulation of the EIC DIRC in GEANT, which will include the interaction of the DIRC with other subsystems of the EIC central detector. This simulation will then be used for the design of the final prototype.
The last stage will see the construction of the final prototype and tests in a particle beam.

3. R&D Timeline

3.1 Year 1

3.1.1 Design and Simulation

Simulation of pion backgrounds in the EIC central detector will determine the need for supplementary e/π discrimination capabilities (beyond the DIRC and EC) in the central detector.

Studies will be carried out of the performance of different expansion volume sizes, shapes, focusing designs, and radiator shapes, in terms of single photon resolution and light yield. The work will comprise:

1. Implementation of initial prototype in GEANT or stand-alone ray-tracing software, including:
    a. Polished fused silica bar/plate
    b. Small 30-cm depth expansion volume
    c. Focusing lens
    d. Multi-pixel readout
2. Development of reconstruction algorithm for the bar/plate geometry.

3.1.2 Hardware

Early results of design/simulation will be used to design the expansion volume prototype. The work will include:

1. Design of a prototype compact EV with multi-pixel readout.
2. Set up DAQ system for readout.
3. Test of EV imaging and sensors using fast laser pulser.

3.1.3 Deliverables

1. Initial e/π identification requirements for the central EIC detector.
2. Simulation and reconstruction framework for DIRC prototype.
3. DIRC resolution studies and initial design of prototype.
4. DAQ system tested using laser pulser.

3.2 Year 2

3.2.1 Design and Simulation

1. Implementation of initial version of EIC DIRC in EIC detector.
2. Interaction between DIRC and other detector components.
    a. material budget
    b. optimize location
3. Initial EIC DIRC performance from physics channels.
    a. establish required performance for "Super-DIRC"
    b. identify areas for performance improvement R&D
4. Design of final EV prototype.

3.2.2 Hardware

1. Setup and installation of high magnetic field sensor testing facility at JLab.
2. Study magnetic field tolerance of SiPM.
3. Test focusing options.
4. Construction of compact EV based on simulation results.
5. Test of prototype and EV with particle beam, if available.

3.2.3 Deliverables

1. Integration of a DIRC into the EIC detector.
2. Performance plots for EIC DIRC.
3. Test of prototype EV.
4. Evaluation of SiPM sensor response in magnetic fields up to 4.7 T.
5. Cherenkov ring resolution in test beam (if available).

3.3.1 Design and Simulation

Final EIC DIRC performance from physics channels.

3.3.2 Hardware

1. Study magnetic field tolerance of MCP-PMT.
2. Design and construction of final EV prototype based on simulation and year 2 results.
3. Test performance with particle beam, if available.

3.3.3 Deliverables

1. Evaluation of MCP-PMT response in magnetic fields up to 4.7 T.
2. Performance parameters of DIRC in the EIC detector.
3. In-beam test of compact EV (if available).
4. Comparison of photon yield for different multi-pixel sensors.
5. Determination of Cherenkov angle resolution of final prototype EV.

4. Management Plan

4.1 Funding Request and Budget

We request a total of $395k over a three year period, as indicated in the tables below. The tables below list the budget broken down by category and recipient.

Budget

	FY11	FY12	FY13	*Total*
Postdoc (50%)	$53,290	$54,000	$55,000	*$162,290*
Students	$8,300	$13,764	$13,764	*$35,828*
Hardware	$41,970	$58,630	$57,200	*$157,800*
Travel	$11,440	$13,606	$14,036	*$39,082*
Total	*$115,000*	*$140,000*	*$140,000*	*$395,000*

	FY11	FY12	FY13	Total
Old Dominion University (ODU)	$53,290	$54,000	$55,000	*$162,290*
Catholic Univesity of America (CUA)	$9,800	$8,300	$8,300	*$26,400*
University of South Carolina (USC)		$7,606	$7,606	*$15,212*
JLab (and GSI through a MoU)	$51,910	$70,094	$69,094	*$191,098*
Total	*$115,000*	*$140,000*	*$140,000*	*$395,000*

Comments

The postdoc and students funding includes university overhead. Matching funds are available for the postdoc. Travel costs include JLab and USC overhead. Hardware costs include JLab overhead.

The FY11 budget of $115k was approved as requested. Compared with the original proposal, slight adjustments were made for FY11 to the postdoc salary due to additional health insurance costs. However, following the advisory committee's recommendations, this was partly offset by reductions in the hardware procurement and travel for that year. The changes in the totals for FY12 and FY13 reflect the expanded scope of the proposal.

4.2 Procurement

Year 1:

1. Materials for CUA undergrad student (computer, etc): $1.5k
2. Dark box for sensor tests: $2k
3. One multi-pixel PMT: $11k
    a. option A: Hamamatsu H9500-03 (256 pixels)
    b. option B: Photonis XP85022 (1024 pixels)
4. SiPMs from several manufacturers: $4k
5. One 6-μm MCP-PMT, round, single anode, BINP, Novosibirsk: $2k
6. Readout electronics: $5k
    a. option A: HADES TRBv2 with TOF-addON, 128 channels with fast TDC (100 ps/count) and time-over-threshold
    b. option B: new, faster version (TRBv3) expected in late 2011 (~10 ps/count, more channels per board), similar cost per channel
7. Cabling for 128 channels: $2.5k
8. Temperature-controlled cool box for SiPM tests: $2k

Total: $30k

Year 2:

1. MCP-PMT or MaMPT with improved photocathode: $15k
2. Add 256 more readout channels: $10k
3. Cabling: $5k
4. Non-magnetic light-tight cool box for high-B sensor tests: $2k
5. Fast pulse generator for the high B-field tests (refurbished old model): $1k
6. High B-field testing equipment (LEDs, fiber optics): $1k
7. SiPMs for high B-field tests from several manufacturers: $3k
8. SiPMs preamplifiers and HV supply (high B-field tests): $4k

Total: $41k

Year 3:

1. Construct very compact EV from solid fused silica: $20k
2. Add one more multi-pixel readout module to the setup (PMT or SiPM, cabling): $20k

Total: $40k

Comment

Most costs are in Euro. A conversion rate of 1.4 USD per 1 Euro is assumed. Listed costs are direct.

4.3 Responsibilities

Following the outline in Section 3, the main responsibility of the US part of the collaboration (CUA, ODU, JLab) will be simulations, design, and integration of the DIRC into the EIC detector. To carry out these tasks, a postdoc (Heghine Seraydaryan) has been hired by ODU, and undergraduate students will be hired at CUA, the latter focusing on the overall detector optimization and performance. The primary responsibility of USC will be to evaluate the performance of SiPMs and MCP-PMTs in magnetic fields

up to 4.7 T. A dedicated facility will be setup at Jefferson Lab under the lead of C. Zorn to perform these tests. JLab will provide the infrastructure, the magnet, most of the readout electronics, and the data acquisition. A graduate student (Tongtong Cao) and undergraduate students from USC will contribute to the installation of the test facility and will perform the sensor tests. The primary responsibility of the German part of the collaboration (GSI) will be to guide the design of the hardware, prototype construction, and carry out a range of tests. The travel support will create opportunities for the US partners (including the postdoc) to take part in the development of the hardware at GSI, and for the German partners to present their results to and participate in the activities of the EIC collaboration.

Appendix A: Development of a High Magnetic-Field Testing Facility at Jefferson Lab and Evaluation of the Tolerance of SiPMs and MCP-PMTs in High Magnetic Fields

1. Project Overview

The performance of two types of readout sensors, SiPMs and MCP-PMTs will be tested in high magnetic fields (up to 4.7 T). Currently, there is no dedicated facility anywhere in the world that allows testing sensors in magnetic fields higher than 2 T. We will perform the tests using a 4.7-T superconducting solenoid magnet that has become available at Jefferson Lab with the end of the 6-GeV program. The dimension of the central bore of the magnet (diameter of 25 cm) allows to design a universal test setup that can become a general facility for sensor studies in high magnetic fields available for EIC related R&D, as well as to the broader physics community.

1.1 Facility Description

- Magnet; The main device of the test facility is the magnet. We will use a superconducting solenoid magnet that has become available at Jefferson Lab with the end of the 6-GeV program. The magnet provides a 4.7-T nominal field at its center point when it is energized at 534 A. The magnitude of the current is controlled and can be set to any desired value up to 534 A. Thus, the magnitude of the magnetic field can be flexibly increased or decreased while keeping the position of the probed device constant. This feature simplifies the design requirements for the test box which will hold the sensors. The equipment necessary to operate the magnet such as cryostat, power supply, controls, holding frame, *etc.*, will also be contributed by the Jefferson Lab. Thus, we do not request any funding for magnet related procurement.
- Test box; Our initial design of a universal non-magnetic, light-tight test box is shown in Fig. 1. It will be made of wood, with the dimensions: 6” x 6” x 8”. The tested sensor will be installed on an opto-mechanical mount that allows for rotation and translation of the sample relative to the magnetic field. The mount itself will be installed on an optical breadboard. The latter allows flexibility in using the box to test multiple/various configurations of sensors or add other elements to the test setup. The design of the lid of the box, with an inner sleeve, ensures a light-tight fit. We will use an LED as a light source. As the sensor will be rotated relative to the field, but the position of the LED will be fixed relative to the sensor, we will cover all the interior surface of the box with a diffuse white coating to allow the sensor to detect a signal independent of its orientation. Non-magnetic, light-tight fittings, mounted on the back side of the box, will be installed for the optical fiber input from the LED, high voltage, low voltage, and output signal. The box will be moved in and out of the magnet’s bore using an aluminum rail mount. The design of the box is suitable for tests of various sensors such as SiPMs, MCP-PMTs, and also PS-PMTs. A test box of the same design, but with different dimensions, was already successfully used by one of us (C. Zorn) for SiPMs tests in magnetic fields up to 1 T at another facility. These previous tests have demonstrated that the proposed design indeed can provide the required functionality such as light tightness, operation in high magnetic field, and the ability to control the sensor orientation with respect to the magnetic field. The test box will feature cooling and temperature control when SiPMs are tested.

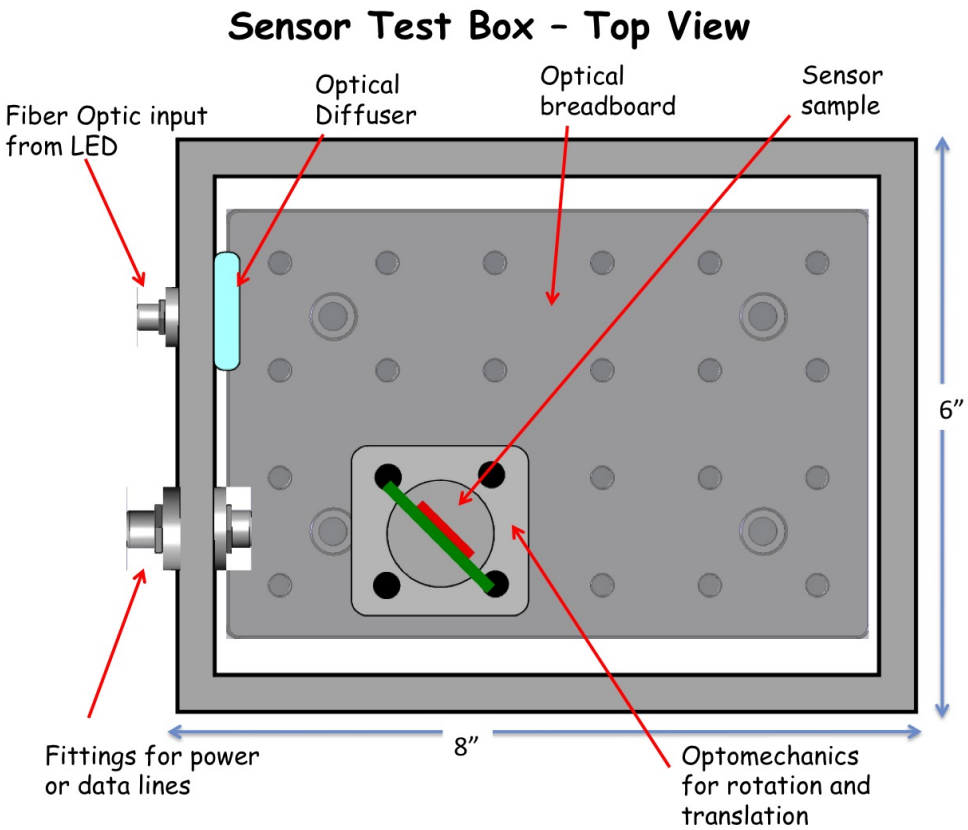

Figure A1: An initial design of a universal non-magnetic, light-tight box to be used for sensor tests in the high magnetic field of the DVCS solenoid magnet. Details of the design are explained in the text.

- Sensors; We will test the high-magnetic-field tolerance of SiPMs and MCP-PMTs. This includes the gain dependence on field magnitude, and gain dependence on field magnitude for various orientations of the sensor with respect to the field lines. We will use the MCP-PMT sensors that were procured under this project during year one. As all of the tests that do not involve high magnetic fields will be done at GSI and there may be difficulties relocating the sensors from Germany to USA and/or back, we propose to acquire an additional set of SiPMs that is to be used for the magnetic-field tests only and will remain permanently at Jefferson Lab.
- Electronics and data acquisition system (DAQ); Most of the readout electronics necessary for the sensor tests is general. Components such as amplifiers, discriminators, scalers, readout controller, and DAQ, are already available at Jefferson Lab. For the set of SiPMs which will be purchased for the high-field tests, we need to procure pulser, custom-built pre-amplifiers and a high-voltage supply.

Jefferson Lab will contribute significantly to the project by providing equipment and facility infrastructure. The Laboratory will provide the magnet and the equipment that is necessary to operate it, most components of the readout electronics, and a laboratory space in a building with a direct supply of liquid helium, where the magnet and the test facility will be installed. The lab space will be available in

the Fall of 2012, which is well in line with the timeline of this project. The design and the construction of the test box will be performed at Jefferson Lab under the lead of C. Zorn. The equipment budget requested here will allow Jefferson Lab to manufacture the test box, and to procure several SiPM sensors for the high B-field tests, fast pulser, LEDs, fiber optics, custom preamplifiers, and HV supply.

1.2 Planned Tests

- SiPMs: For a fixed angle of the sensor plate with the magnetic field lines, we will map the amplitude of the output signal at various magnetic fields up to 4.7 T. We will extend these studies on sensors with various levels of radiation damage.
- MCP-PMTs: We will map the gain change of the sensors at various magnetic fields up to 4.7 T and various orientations of the sensors relative to the field lines. Previous studies of these sensors up to 2 T suggest that the amplitude of the output signal deteriorates due to the effect of the magnetic field on the trajectory of the avalanche electrons. In addition to introducing small-diameter MCPs (our focus will be on sensors with pore size in the range of 6 - 10 μm), a partial compensation of the loss of signal can be achieved by increasing the high voltage on the PMTs above the nominal working high voltage. We will establish the most optimal working high voltages to operate the MCP-PMTs for various strengths of magnetic field. As the wavelength of the incident light affects the kinetic energy of the photoelectron and the kinetic energy is not affected by the magnetic field, we do not expect the response of the sensor in different magnetic fields to also vary with incident light wavelength. However, as we determine the most optimal working voltage for the sensor, and that may depend on the field magnitude, there may be wave-length dependent effects. In order to study any such effects, we will initially use only two types of light: blue and green. If we find that the response of the sensor in various fields also depends on the input-light wavelength, we will extend the tests to include wavelength dependence.

1.4 Broader impact

A high-magnetic field testing facility for sensor studies is of interest to a broad community. Currently, there is no research facility providing magnetic fields above 2 T. In order to test sensors in higher fields, one needs to negotiate access to magnets at clinical facilities. The latter have two aspects of inflexibility. First, access is not readily available and, if granted, it is very limited. Second, clinical magnets operate at fixed current, so that evaluating the sensor response over a range of magnetic fields requires complicated design solutions. For example, the probed sensor must be moved within the magnet in order to access locations with different field strength than the nominal one, and the setup must provide means to measure the field at the location of the sample. The ability to control the strength of the magnetic field in our setup is, thus, a great advantage. The relatively large diameter of the central bore of the magnet allows for the design of a universal light-tight box which can house sensors of various geometry and size. Once established, we envision that the high-magnetic field testing facility at Jefferson Lab will have a long-lasting value for sensor studies beyond nuclear-physics applications. For instance, there is a growing interest to use SiPMs as readout elements in scintillator-based positron emission tomography (PET), particularly for small-animal or organ-specific imaging. The feasibility of SiPMs for such systems is currently ongoing. Specifically, a high B-field sensor testing facility can be useful for the development of combined PET/MRI scanners that use SiPMs.

Appendix B: Short Project Status Summary

1. FY11

1.1 General

An addendum to the FY11 proposal was provided, incorporating an initial response to the Advisory Committee's comments and suggestions. In particular, the FY11 work was shifted entirely from prototype construction towards simulations and studies of sensor capabilities.

The FY11 contracts were set up between BNL and JLab/ODU/CUA from mid August to early September 2011, and the funding became available shortly thereafter.

1.2 Hardware

A MoU has been signed between JLab and GSI, making it possible to proceed with quotes from the identified vendors, and eventually initiate procurement of the FY11 hardware.

1.3 Simulations and Design of the DIRC Readout

The ODU postdoc (H. Seraydaryan) was hired in early November. Her position will be 100% dedicated to the EIC R&D for November 2011 - March 2012, and 50% thereafter.

DIRC ray-tracing software (drcprop) has been transferred from GSI to JLab, and work has started on the simulation of the propagation of Cherenkov light in the Silica bars and readout volume. Computer accounts have been set up at JLab for the GSI collaborators to provide further direct support.

In parallel, efforts have started on adapting the MEIC GEANT4 package (GEMC), which is also the standard simulation package for CLAS12, to simulate the DIRC detector, initially in a standalone mode, but with the goal of eventually including the other EIC detector elements. GSI will provide help with algorithms and methods based on GEANT simulations used for the PANDA DIRC.

1.4 Backgrounds

Radiation background studies were continued in collaboration with M. Sullivan from SLAC and the JLab accelerator group. In particular, a mini-workshop was held at JLab October 31 - November 4, a major goal of which was to quantify the synchrotron radiation and gamma-induced fluxes. Work was also started on the layout of the vacuum systems, which is required for a detailed simulation of the backgrounds due to residual gas. The initial evaluation of the JLab design seemed quite promising. We hope to initiate similar contacts with the BNL accelerator group in the near future.

This group is also actively involved with the larger JLab EIC design effort to detail the IP optics, which impacts both the physics program and particle background in the central detector.

2. FY12 and FY13

2.1 Sensor Tests in High Magnetic fields

Following the suggestions of the Advisory Committee, a plan has been put in place for setting up a high magnetic field sensor testing facility at JLab, together with C. Zorn and collaborators at JLab, and the University of South Carolina. The details are outlined in Appendix A.